



Original Research

A multigene circulating biomarker to predict the lack of FOLFIRINOX response after a single cycle in patients with pancreatic ductal adenocarcinoma



Casper W.F. van Eijck^{a,b}, Willem de Koning^{b,c}, Fleur van der Sijde^{a,b},
Miranda Moskie^a, Bas Groot Koerkamp^a, Marjolein Y.V. Homs^d,
Sjoerd H. van der Burg^e, Casper H.J. van Eijck^{a,b}, Dana A.M. Mustafa^{b,*}

^a Department of Surgery, Erasmus University Medical Center Rotterdam, 3000 CA Rotterdam, the Netherlands

^b Department of Pathology Unit of Tumour Immuno-Pathology, Erasmus University Medical Center Rotterdam, 3000 CA Rotterdam, the Netherlands

^c Department of Pathology Unit of Clinical Bioinformatics, Erasmus University Medical Center Rotterdam, 3000 CA Rotterdam, the Netherlands

^d Department of Medical Oncology, Erasmus University Medical Center Rotterdam, 3000 CA Rotterdam, the Netherlands

^e Department of Medical Oncology, Oncode Institute, Leiden University Medical Center, 2300 RC Leiden, the Netherlands

Received 22 December 2022; accepted 23 December 2022

Available online 28 December 2022

KEYWORDS

Pancreatic ductal adenocarcinoma (PDAC); FOLFIRINOX chemotherapy; Lack of response; Blood immune transcriptome; FFX-ΔGEP score; Precision medicine

Abstract Introduction: 5-fluorouracil, folinic acid, irinotecan and oxaliplatin (FOLFIRINOX) is promising in treating patients with pancreatic ductal adenocarcinoma. However, many patients and physicians are reluctant to start FOLFIRINOX due to its high toxicity and limited clinical response rates. In this study, we investigated the effect of a single FOLFIRINOX cycle, in combination with a granulocyte colony-stimulating factor, on the blood immune transcriptome of patients with pancreatic ductal adenocarcinoma. We aimed to identify an early circulating biomarker to predict the lack of FOLFIRINOX response.

Methods: Blood samples of 68 patients from all disease stages, who received at least four FOLFIRINOX cycles, were collected at baseline and after the first cycle. The response to treatment was radiologically evaluated following the Response Evaluation Criteria in Solid Tumours criteria 1.1. Targeted immune-gene expression profiling (GEP) was performed using NanoString technologies. To predict the lack of FOLFIRINOX response, we developed a FOLFIRINOX delta GEP (FFX-ΔGEP) score.

* Corresponding author: P.O. Box 2040, 3000 CA Rotterdam, the Netherlands.

E-mail address: c.w.f.vaneijck@erasmusmc.nl (C.W.F. van Eijck), w.dekoning.1@erasmusmc.nl (W. de Koning), f.vandersijde@erasmusmc.nl (F. van der Sijde), m.moskie@erasmusmc.nl (M. Moskie), b.grootkoerkamp@erasmusmc.nl (B. Groot Koerkamp), m.homs@erasmusmc.nl (M.Y. V. Homs), S.H.van_der_Burg@lumc.nl (S.H. van der Burg), c.vaneijck@erasmusmc.nl (C.H.J. van Eijck), d.mustafa@erasmusmc.nl (D.A.M. Mustafa).

Results: A single FOLFIRINOX cycle significantly altered 395 genes, correlating to 30 significant alterations in relative immune cell abundances and pathway activities. The eight-gene (*BID*, *FOXP3*, *KIR3DL1*, *MAF*, *PDGFRB*, *RRAD*, *SIGLEC1* and *TGFB2*) FFX-ΔGEP score predicted the lack of FOLFIRINOX response with a leave-one-out cross-validated area under the curve (95% confidence interval) of 0.87 (0.60–0.98), thereby outperforming the predictiveness of absolute and proportional Δcarbohydrate antigen19-9 values.

Conclusions: A single FOLFIRINOX cycle, combined with granulocyte colony-stimulating factor, alters the peripheral immune transcriptome indisputably. Our novel FFX-ΔGEP is, to our knowledge, the first multigene early circulating biomarker that predicts the lack of FOLFIRINOX response after one cycle. Validation in a larger independent patient cohort is crucial before clinical implementation.

© 2022 The Authors. Published by Elsevier Ltd. This is an open access article under the CC BY license (<http://creativecommons.org/licenses/by/4.0/>).

List of abbreviations

AUC	Area Under the Curve	ISG15	Interferon-Stimulated Gene 15
BH.P	Benjamin-Hochberg corrected <i>P</i> value	KIR3DL1	Killer Cell Immunoglobulin Like Receptor 3DL1
BID	BH3-Interacting Domain Death Agonist	LAG3	Lymphocyte Activating Gene 3
BTLA	B and T Lymphocyte Associated	LAPC	Locally Advanced Pancreatic Cancer
CA19–9	Cancer antigen 19-9	LASSO	Least Absolute Shrinkage and Selection Operator
CD	Cluster of Differentiation	Lipegfilgrastim	glycoPEGylated human N-methionyl granulocyte-colony stimulating factor
CD86 (B7-2)	CD86 Antigen (CD28 Antigen Ligand 2, B7-2 Antigen)	MAF	Avian Musculoaponeurotic Fibrosarcoma
CD274 (PD-L1)	Programmed Cell Death Ligand 1	OAS3	2'-5'-Oligoadenylate Synthetase 3
cDC2s	conventional Dendritic Cells type 2	OS	Overall survival
CI	Confidence Interval	PDAC	Pancreatic Ductal Adenocarcinoma
CT	Computed Tomography	PDCD1 (PD-1)	Programmed Cell Death 1
CTLA4	Cytotoxic T-Lymphocyte Associated protein 4	PDCD1LG2 (PD-L2)	Programmed Cell Death Ligand 2
DEGs	Differentially Expressed Genes	PDGFRB	Platelet-Derived Growth Factor Receptor β
ELISA	Enzyme-Linked Immunosorbent Assay	PTPRC	Protein Tyrosine Phosphatase Receptor Type C
FFX-ΔGEP score	FOLFIRINOX delta Gene Expression Profiling score	RRAD	Ras-Related Associated with Diabetes
FOC	Fold-Of-Change	RECIST	Response Evaluation Criteria In Solid Tumors
FOLFIRINOX	Regimen of 5-fluorouracil, folinic acid, irinotecan, and oxaliplatin	ROC	Receiver Operating Curve
FOV	Fields Of View	SIGLEC1 (CD196)	Sialic Acid Binding Ig Like Lectin 1
FOXP3	Forkhead Box P3	TGFB2	Transforming growth factor β 2
G-CSF	Granulocyte-colony stimulating factor	TIGIT	T cell Immunoreceptor with Ig and ITIM domains
HAVCR2 (TIM-3)	Hepatitis A Virus Cellular Receptor 2	TLR	Toll-Like Receptor
IC	Immune Checkpoint	TME	Tumour Microenvironment
IFN-I	Interferon-I	TNF	Tumour Necrosis Factor
		Treg	T regulatory cell

1. Introduction

Pancreatic ductal adenocarcinoma (PDAC) is one of the most lethal and aggressive solid malignancies with a poor prognosis [1,2]. The 5-year overall survival (OS) rate for all stages of PDAC is only 9% [3]. The poor prognosis is, among other things, related to the lack of distinctive symptoms, the lack of reliable biomarkers for early diagnosis, progressive metastatic spread and the complex tumour (immune) microenvironment [4]. Surgical resection with or without chemotherapy is the only

curative treatment for early-stage PDAC, but only 20% of the tumors are resectable at diagnosis, and more than 50% of patients present with metastatic disease [5–7].

The combined chemotherapeutic regimen of 5-fluorouracil, folinic acid, irinotecan and oxaliplatin (FOLFIRINOX) is considered one of the most effective adjuvant chemotherapy and first-line treatment for patients with locally advanced pancreatic cancer (LAPC) and metastatic pancreatic cancer [8]. Multiple studies have demonstrated that FOLFIRINOX treatment is associated with prolonged OS compared to gemcitabine

treatment in all stages of the disease [9–11]. A meta-analysis combining 11 studies reported improved OS in LAPC (24.2 months versus 6–13 months) [9]; a multicenter, randomised, phase 2–3 trial reported improved OS in metastatic patients (11.1 months versus 6.8 months) [10]; a multicenter, randomised, phase 3 trial reported the most prolonged OS in patients with stage I–II or borderline resectable patients [11]. In addition, neoadjuvant FOLFIRINOX followed by surgical resection showed favourable outcomes in patients having resectable pancreatic cancer [12]. Despite the generally improved FOLFIRINOX response rates, 25% of patients having PDAC experience disease progression during treatment [10,13].

FOLFIRINOX treatment has also been associated with a higher incidence of toxicity-related events than gemcitabine treatment [10,14]. To prevent FOLFIRINOX-induced neutropenia, patients are frequently treated with a prophylactic granulocyte colony-stimulating factor (G-CSF) which stimulates granulocyte production in the bone marrow [15–18]. Currently, treatment response is evaluated through computed tomography (CT) imaging, but not until after four cycles of FOLFIRINOX. Exposure to ineffective but toxic treatment reduces patients' quality of life, carries unnecessary costs and withholds patients from a potentially effective treatment. Hence, it is desirable to identify a biomarker that predicts the lack of response to FOLFIRINOX at an early stage. Carbohydrate antigen 19-9 (CA19-9) is the only FDA-approved biomarker for the routine management of PDAC [19] but has only been shown to predict FOLFIRINOX response after multiple cycles [20].

Several studies have demonstrated that oxaliplatin, 5-FU and irinotecan can enhance tumour antigen presentation in poor immunogenic cancer types such as PDAC [21,22]. The increase in HLA-I and programmed death-ligand 1 could synthesize the tumour for immune checkpoint (IC)-based immunotherapy and stimulates CD8⁺ cytotoxic T lymphocyte activation [23]. Particularly, oxaliplatin has been shown to induce immunogenic cancer cell death and modulate the immune response, resulting in increased antigenicity and enhanced adaptive immune responses [24–26]. Additionally, oxaliplatin has been shown to elicit a systemic immune response against the tumour [27]. However, the peripheral immune effects of FOLFIRINOX have not been studied.

We hypothesised that the immune-modulating effects of FOLFIRINOX may be detectable in the peripheral blood after a single cycle of treatment. To test this hypothesis, we conducted targeted immune-gene expression profiling on the blood of patients with PDAC. The aim of this study was to investigate the impact of a single FOLFIRINOX cycle on the peripheral immune transcriptome and identify an early circulating

biomarker predictive of the lack of FOLFIRINOX response in patients with PDAC.

2. Methods

2.1. Patient population

A total of 80 patients with PDAC were included in this study. Patients were hospitalised at the Erasmus University Medical Centre Rotterdam between February 2018 and February 2021. Twenty-three patients with (borderline) resectable PDAC participated in the randomised clinical trial PREOPANC-2 (Dutch trial register NL7094), and 57 patients with locally advanced or metastasised PDAC participated in the prospective cohort study iKnowIT (Dutch trial register NL7522). Exclusion criteria were <18 years of age, previous treatment with FOLFIRINOX or co-treatment with another chemotherapeutic.

2.2. Clinical procedure

Following histological confirmation of the primary tumour or metastases, patients were treated with FOLFIRINOX chemotherapy. All patients were prophylactically treated with the long-acting G-CSF lipegfilgrastim (Lonquex[®]; Teva Ltd, Petach Tikva, Israel), 24 h after each cycle, to reduce FOLFIRINOX-induced neutropenia [18,28]. Two whole blood samples from each patient were collected: at baseline (immediately before the first cycle) and 14 days after the first but just before the second FOLFIRINOX cycle. As part of the standard clinical routine, serum CA19-9 concentrations were determined at the same time points using an enzyme-linked immunosorbent assay. A patient's response to FOLFIRINOX was assessed based on a CT scan made after four cycles, following the Response Evaluation Criteria in Solid Tumours 1.1 criteria (Fig. 1) [29].

2.2.1. Clinicopathological groups

To compare immune profiles, patients were grouped based on their clinicopathological characteristics. Disease stages at baseline included resectable, LAPC and metastatic patients. Baseline CA19-9 values included patients with low (35–150 $\mu\text{mol/L}$) and high (>1500 $\mu\text{mol/L}$) values. Patients who showed stable disease, partial response or complete radiological response were defined as 'disease control'. Patients showing disease progress were defined as 'progressive disease'. All patients that were radiologically evaluated received at least four cycles of FOLFIRINOX.

2.3. Whole blood sample collection and RNA isolation

Whole blood samples were collected in Tempus tubes (Applied Biosystems, Foster City, CA, USA) and stored

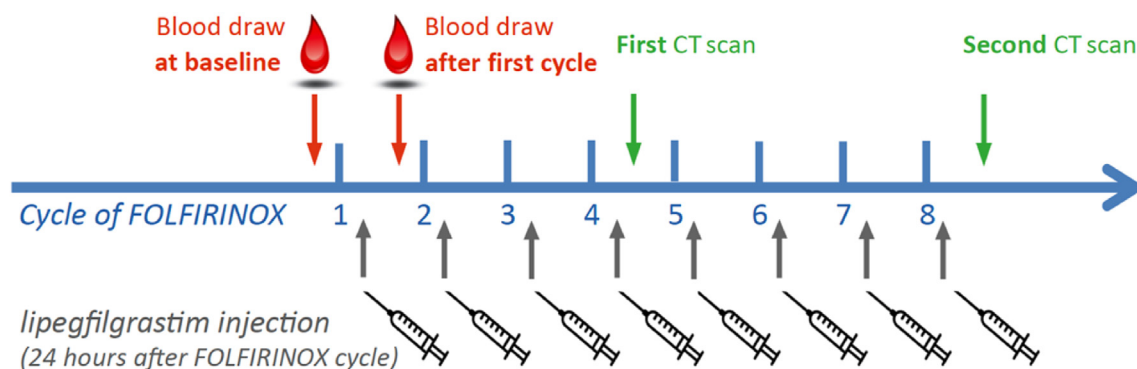


Fig. 1. **Schematic description of clinical procedure.** Cycles of FOLFIRINOX chemotherapy (blue), lipegfilgrastim injection 24 h after each cycle (grey), blood draw time points (red) and patient evaluation time points using CT scan (green). (For interpretation of the references to colour in this figure legend, the reader is referred to the Web version of this article). CT, computed tomography; FOLFIRINOX, 5-fluorouracil, folinic acid, irinotecan and oxaliplatin.

at -80°C . Tempus tubes contain an RNA stabilizing reagent, which preserves the RNA quality and enables measuring gene expression profiles without isolating the peripheral blood mononuclear cells [30]. Total RNA was extracted from blood in Tempus tubes using the Tempus Spin RNA Isolation Kit of Thermo Fisher Scientific (Waltham, MA, USA) following the manufacturer's instructions. RNA quality control was done using the Agilent 2100 BioAnalyzer (Santa Clara, CA, USA). Samples with RNA concentrations less than 35 mg/mL were excluded. Corrected RNA concentrations were calculated based on the percentage of fragments of 300–4000 nucleotides to correct RNA degradation.

2.4. Targeted multiplex gene expression

Targeted gene expression profiling was performed using the nCounter[®] FLEX system and PanCancer Immune profiling panel, which includes 40 housekeeping genes and 730 immune-related genes [31]. A total of 200 ng RNA per sample in a maximum of 7 μL was used for hybridisation, which was performed at 65°C for 17 h using the SimpliAmp Thermal Cycler (Applied Biosystems). Gene expression was counted by scanning 490 Fields of View.

2.4.1. Data processing and analysis

Data quality control, normalisation and analysis were performed using the nSolver[™] software (version 4.0) and the advanced analysis module (version 2.0) of NanoString Technology Inc [32]. A patient's gene expression profile was included if all positive and negative control genes were within the expected values and if binding density values ranged between 0.5 and 3.0. Raw gene counts were normalised based on the most stable 34 housekeeping genes, identified by the geNorm algorithm [33], and all normalised data were \log_2 transformed. Genes were included when they were

higher than the limit of detection of $4.384 \log_2$, calculated as the average of all eight negative control genes multiplied by two, in $>80\%$ of the gene expression profiles. Differentially expressed genes (DEGs) were identified using simplified negative binomial models, a mixture of negative binomial models or log-linear models based on the convergence of each gene. Genes with a P-value <0.05 after correction for multiple testing with the Benjamin–Hochberg (BH) method were considered DEGs.

2.4.2. Immune cell type analysis with the NanoString nSolver module

The peripheral abundance of various immune cell types was quantified using the nSolver advanced analysis module, which assigns relative immune cell type scores to each sample [34]. Marker genes, that identify specific immune cell types, were selected based on the pairwise similarities method tailored specifically for PDAC [35]. Marker genes were accepted to define an immune cell type when pairwise similarity was sufficient ($R^2 \geq 0.6$). Accordingly, the relative abundance of immune cells was calculated between the tested groups (Table S2).

2.4.3. Pathway analysis with the NanoString nSolver module and the cytoscape plug-in ClueGO

Genes were clustered into predefined pathways using the nSolver advanced analysis module to examine the immune-associated pathway alterations. We calculated the square root of the average squared t-statistic of all genes in the corresponding pathway [34], resulting in a pathway score for each sample. In addition, to explore the potential role of unique DEGs in disease control and progressive disease patients, we performed functional enrichment analysis using the Cytoscape plug-in ClueGO [36]. DEGs were included in the ClueGO analysis if they met two criteria: (1) a \log_2 fold-of-change (FOC) $> |0.5|$ after a single FOLFIRINOX

cycle and (2) a \log_2 FOC $> |0.5|$ difference between disease control and progressive disease patients.

2.5. Statistical analysis

Statistical testing and data visualisation were performed with R Statistical Software (v.4.1.2) [37]. Data were tested for normality with Shapiro–Wilk tests. We used paired or unpaired two-sided student t-tests for parametrical data and paired Wilcoxon tests or unpaired Mann–Whitney U tests for non-parametrical data. All tests were corrected with the BH correction for multiple testing. We used the R packages ggplot2 [38] and EnhancedVolcano [39] for data visualisation.

2.6. The FOLFIRINOX delta gene expression profiling score

A gene signature representing an early predictive circulating biomarker of the lack of FOLFIRINOX response was identified (the FFX- Δ GEP score). Briefly, \log_2 normalised gene expression counts of baseline samples were subtracted from the \log_2 normalised gene expression counts of samples after a single FOLFIRINOX cycle, resulting in Δ expression counts for each gene. Genes that showed statistically significant differences (BH.P < 0.05) in Δ expression count between disease control and progressive disease patients were identified as candidate genes for the FFX- Δ GEP score. Patients were randomly split into training and test sets (75%/25%). To find the combination of candidate genes predicting the lack of FOLFIRINOX response most accurately, the least absolute shrinkage and selection operator multivariate regression analysis was conducted on the training set with leave-one-out cross-validation. Weights (regression coefficient) were assigned to the candidate genes to improve model robustness and avoid overfitting. Genes weighted with a regression coefficient of 0 were excluded from the FFX- Δ GEP score. The fitted model was used in the corresponding test set to predict the lack of FOLFIRINOX response. The overall predictive performance was assessed by receiver operating characteristic (ROC) analysis depicting the area under the curve (AUC) value with a 95% confidence interval (CI).

The absolute ($\mu\text{mol/L}$) and proportional (%) change in CA19-9 was calculated to compare the predictive performance to the FFX- Δ GEP score. CA19-9 values of baseline samples were subtracted from those after a single FOLFIRINOX cycle to obtain absolute Δ CA19-9 values. The proportional Δ CA19-9 values were calculated by dividing the absolute Δ CA19-9 values by their baseline Δ CA19-9 values. ROC analysis was performed for both absolute and proportional Δ CA19-9 values, and the AUC value was compared to the AUC value of the FFX- Δ GEP score.

3. Results

3.1. Samples and patient characteristics

Blood samples from 80 patients were collected at baseline and after the first cycle (Fig. 1). RNA isolation was performed for all 160 blood samples. However, eight were excluded due to poor RNA concentration (< 35 mg/mL) and four were excluded due to poor binding density (< 0.5 or > 3.0). After removing corresponding pairs, 68 patients (136 samples) were included in the data analysis. The response to four FOLFIRINOX cycles was assessed by CT scan evaluation in 58 out of 68 patients, which resulted in 48 disease control and 10 progressive disease patients. No CT scan was performed in ten patients due to toxicity or early progression during FOLFIRINOX treatment. The OS (95% CI) for the disease control and the progressive disease patients was 40.2 months (32.7–46.5) and 13.8 months (11.2–15.5). All clinicopathological characteristics are summarised in Table 1.

3.2. PDAC patients with different disease stages or different baseline CA19-9 values show comparable immune profiles

Immune profiles based on the three disease stages (resectable, LAPC and metastatic) and based on the two baseline CA19-9 values (low and high) were compared at baseline and after a single FOLFIRINOX cycle. Baseline immune profiles revealed eight DEGs between the three disease stages and no DEGs between low and high baseline CA19-9 values (Figure S1). The pathway activity in baseline samples was not altered in any of the comparisons (BH.P > 0.05). Two immune cell types were relatively different between the three disease stages (BH.P < 0.05). Resectable patients showed relatively lower NK cells than LAPC and metastatic patients, and relatively lower conventional dendritic cells type 2 (cDC2s) than metastatic patients (BH.P < 0.05). No immune cell types were relatively different between the two baseline CA19-9 values (BH.P > 0.05 ; Figure S1).

A single FOLFIRINOX cycle induced multiple DEGs amongst the three disease stages and the two baseline CA19-9 values (Figure S2). However, unique DEGs between groups were scarce, resulting in six statistically significant differences (BH.P < 0.05) in altered pathways and immune cell type abundances (Figure S3). The cytotoxicity pathway was less activated in metastatic compared to resectable patients (BH.P < 0.05). The relative cytotoxic cell abundance was higher in metastatic than resectable and LAPC patients (BH.P < 0.05). Additionally, patients with high baseline CA19-9 values showed relatively higher neutrophils and NK CD56^{dim} cells and relatively lower monocytes than patients with low CA19-9 values (BH.P < 0.05 ; Figures S3 and S4).

Table 1
Clinicopathological characteristics of patients in the study.

	All patients	Treatment response	
	(n = 68)	Disease control (n = 48)	Progressive disease (n = 10)
Age (y), mean (range)	65 (47–81)	65 (49–78)	60 (47–69)
Sex, no (%)			
Male	35 (51%)	25 (52%)	5 (50%)
Female	33 (49%)	23 (48%)	5 (50%)
Alcohol, no (%)			
Yes	35 (51%)	22 (46%)	3 (30%)
No	33 (49%)	26 (54%)	7 (70%)
Smoking, no (%)			
Yes	40 (59%)	28 (58%)	6 (60%)
No	28 (41%)	20 (42%)	4 (40%)
Diabetes Mellitus (DM), no (%)			
Yes	14 (11%)	11 (33%)	2 (20%)
No	54 (79%)	37 (77%)	8 (80%)
Disease stage, no (%)			
Resectable disease	21 (31%)	17 (35%)	2 (20%)
LAPC	28 (41%)	19 (40%)	5 (50%)
Metastatic disease	19 (28%)	12 (25%)	3 (30%)
Baseline CA19–9 (U/mL), no (%)			
Mean (\pm SD)	2919 (\pm 10893)	1352 (\pm 4182)	10503 (\pm 25859)
No expression (<35)	13 (19%)	9 (19%)	3 (30%)
Low expression (35–150)	15 (22%)	13 (27%)	0 (0%)
Moderate expression (150–1500)	25 (37%)	19 (39.5%)	3 (30%)
High expression (>1500)	15 (22%)	7 (14.5%)	4 (40%)
CA19–9 difference after a single cycle, compared to baseline			
Mean (U/mL) (\pm SD)	225.5 (\pm 1883)	128.1 (\pm 1777)	242.5 (\pm 2042)
Mean (%) (range)	15 (-62 – 304)	20% (-53 – 304)	5% (-62 – 49)
Baseline clinical parameters, mean (\pmSD)			
CEA (μ g/L)	19.09 (\pm 49)	11.86 (\pm 24)	32.70 (\pm 69)
Bilirubin (μ mol/L)	13 (\pm 12)	13 (\pm 8.0)	20 (\pm 23)
CRP (mg/L)	16 (\pm 24)	17 (\pm 25)	17 (\pm 24)
SII	1182 (\pm 1151)	1116 (\pm 1067)	1189 (\pm 713)
NLR	4.0 (\pm 2.8)	4.0 (\pm 3.0)	3.8 (\pm 1.8)
Total cycles of FOLFIRINOX, mean (\pmSD)	7.0 (\pm 3.0)	8.0 (\pm 2.0)	4.0 (\pm 2.0)
Median OS (months), mean (\pmSD)	11.7 (\pm 6.6)	13.0 (\pm 5.2)	8.27 (\pm 7.3)

Overall survival (OS) is defined as the difference in months (\pm SD) between the first FOLFIRINOX cycle and the date of death.

Abbreviations LAPC: Locally Advanced Pancreatic Cancer; CA19-9: Carbohydrate Antigen 19-9; CEA: Carcinoembryonic Antigen; CRP: C-Reactive Protein; SII: Systemic Immune-inflammation Index; NLR: Neutrophil-to-Lymphocyte Ratio; SD: Standard Deviation; OS: Overall Survival.

3.3. A single FOLFIRINOX cycle altered the peripheral immune transcriptome of PDAC patients

Data analysis revealed 395 DEGs (BH.P < 0.01) in samples after a single FOLFIRINOX cycle compared to baseline samples (Fig. 2A). Filtering the DEGs based on a \log_2 FOC \geq |1.0| revealed 36 upregulated genes and

three downregulated genes after a single FOLFIRINOX cycle (Fig. 2B). Pathway analysis revealed alterations among all immune-associated pathways (BH.P < 0.001; Fig. 3A–C). Pathway-specific genes with \log_2 FOC \geq |1.0| were considered key pathway drivers (Table S1). The pathways of adhesion, chemokines, cytokines, interleukins, macrophage function, pathogen defense, toll-

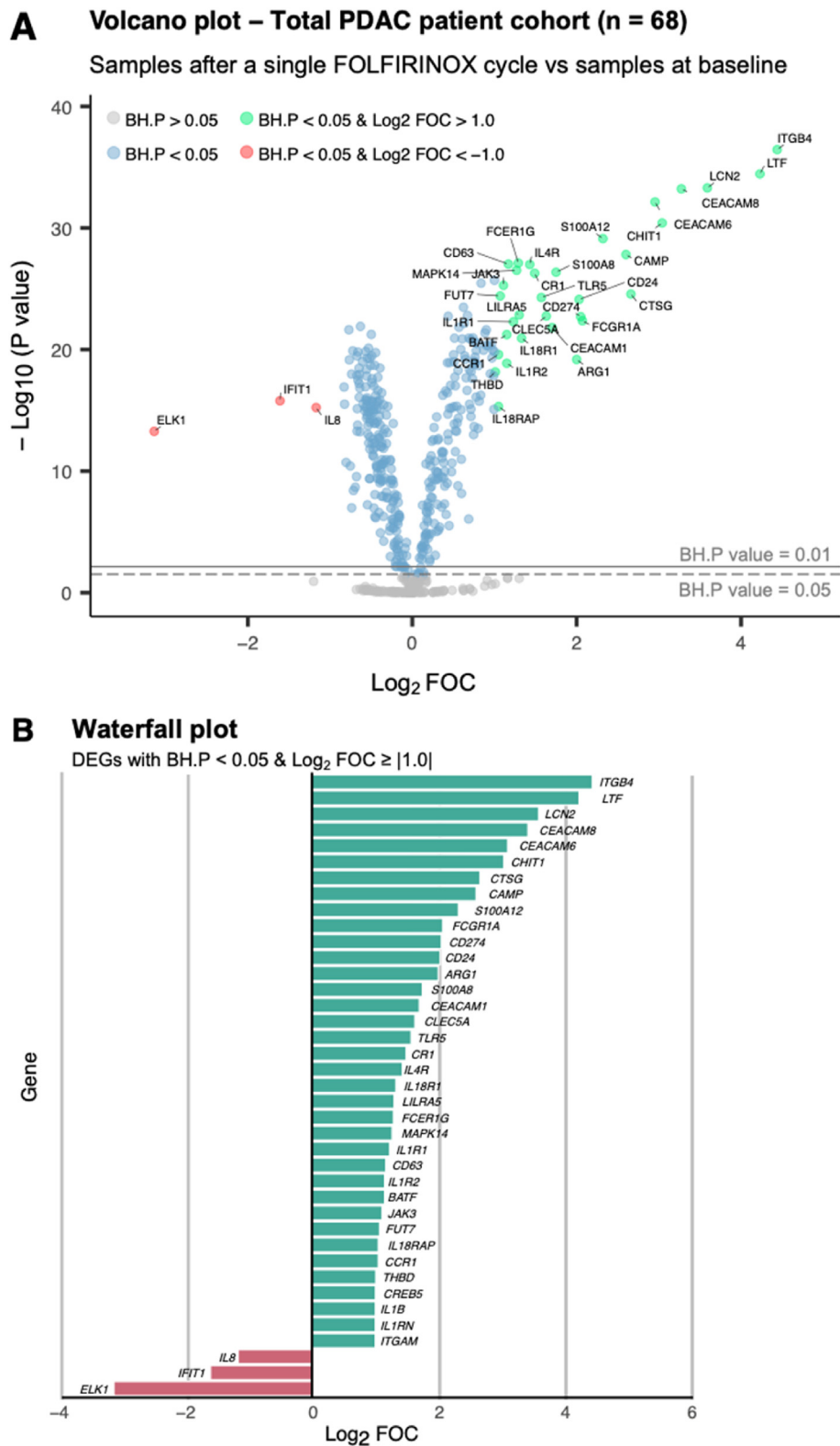


Fig. 2. **Identified DEGs after a single FOLFIRINOX cycle.** (A): Volcano plot of the identified DEGs using the paired analysis embedded in the Advanced Analysis module. Each dot is a gene, all DEGs genes (blue), upregulated DEGs with FOC < -1.0 in baseline samples (red), upregulated DEGs with FOC >1.0 in samples after a single FOLFIRINOX cycle (green) and non-significant genes (grey). (B): Waterfall plot displaying DEGs of BH.P < 0.05 and Log₂ FOC ≥ |1.0|. Upregulated DEGs with FOC < -1.0 in baseline samples (red), and upregulated DEGs with FOC >1.0 in samples after a single FOLFIRINOX cycle (green). *Abbreviations:* BH.P: Benjamin–Hochberg P value; DEG, differentially expressed gene; FOC: Fold Of Change.

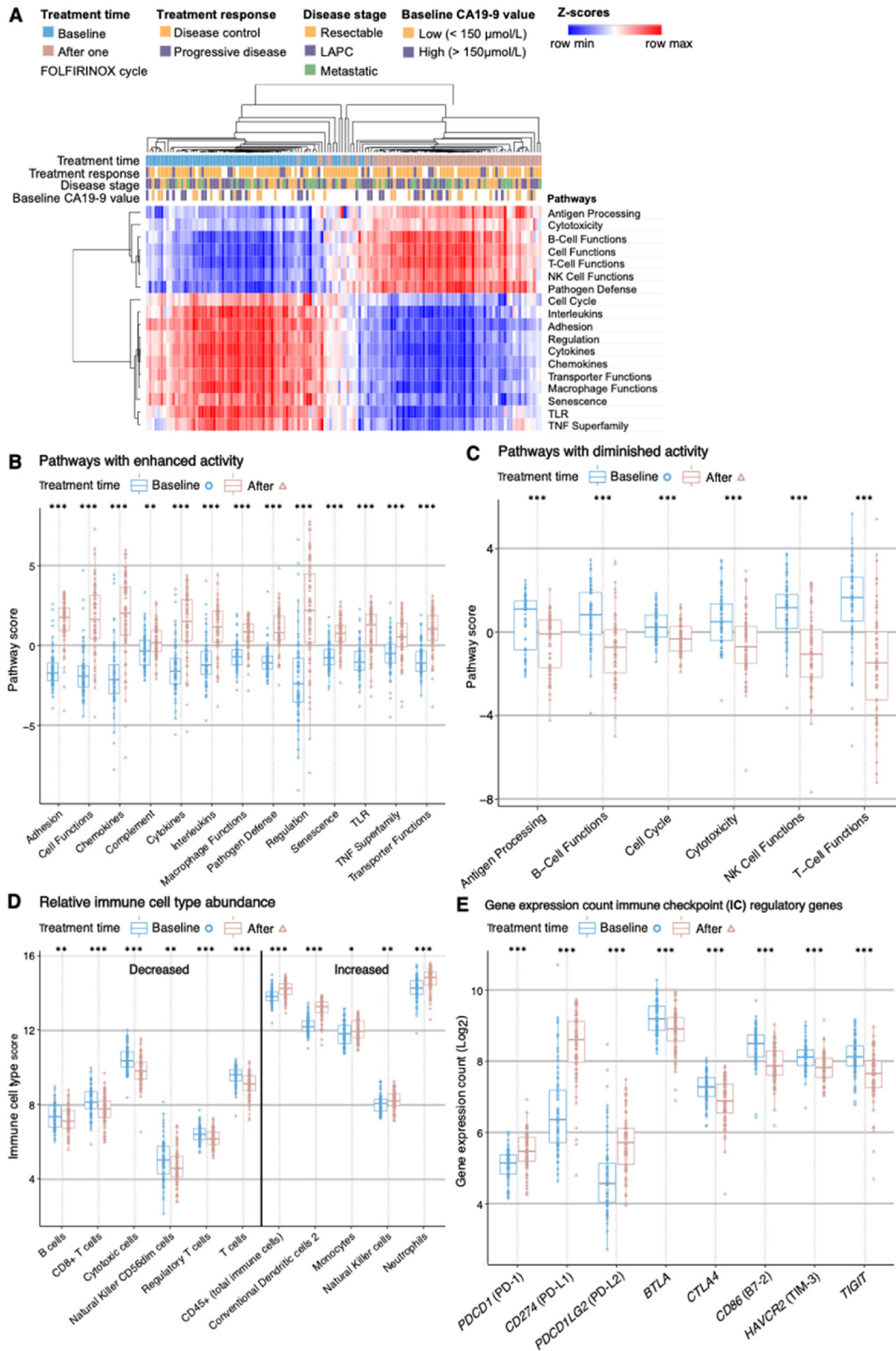


Fig. 3. Immune profile alterations after a single FOLFIRINOX cycle. Samples at baseline (blue) and after one FOLFIRINOX cycle (brown). (A): Heatmap of pathway scores showing sample clustering based on time of collection. (B) and (C): Boxplots of pathways with enhanced (B) and diminished (C) activity. (D): Boxplots of relative immune cell type abundance. (E): Boxplots of IC regulatory genes. Statistical significance: *BH.P < 0.05, ***BH.P < 0.001. Abbreviations: NK: natural killer; TLR: toll-like receptor; TNF: tumor necrosis factor; BH.P: Benjamin–Hochberg P value; FOLFIRINOX, 5-fluorouracil, folinic acid, irinotecan and oxaliplatin; IC: immune checkpoint; PD: programmed cell death.

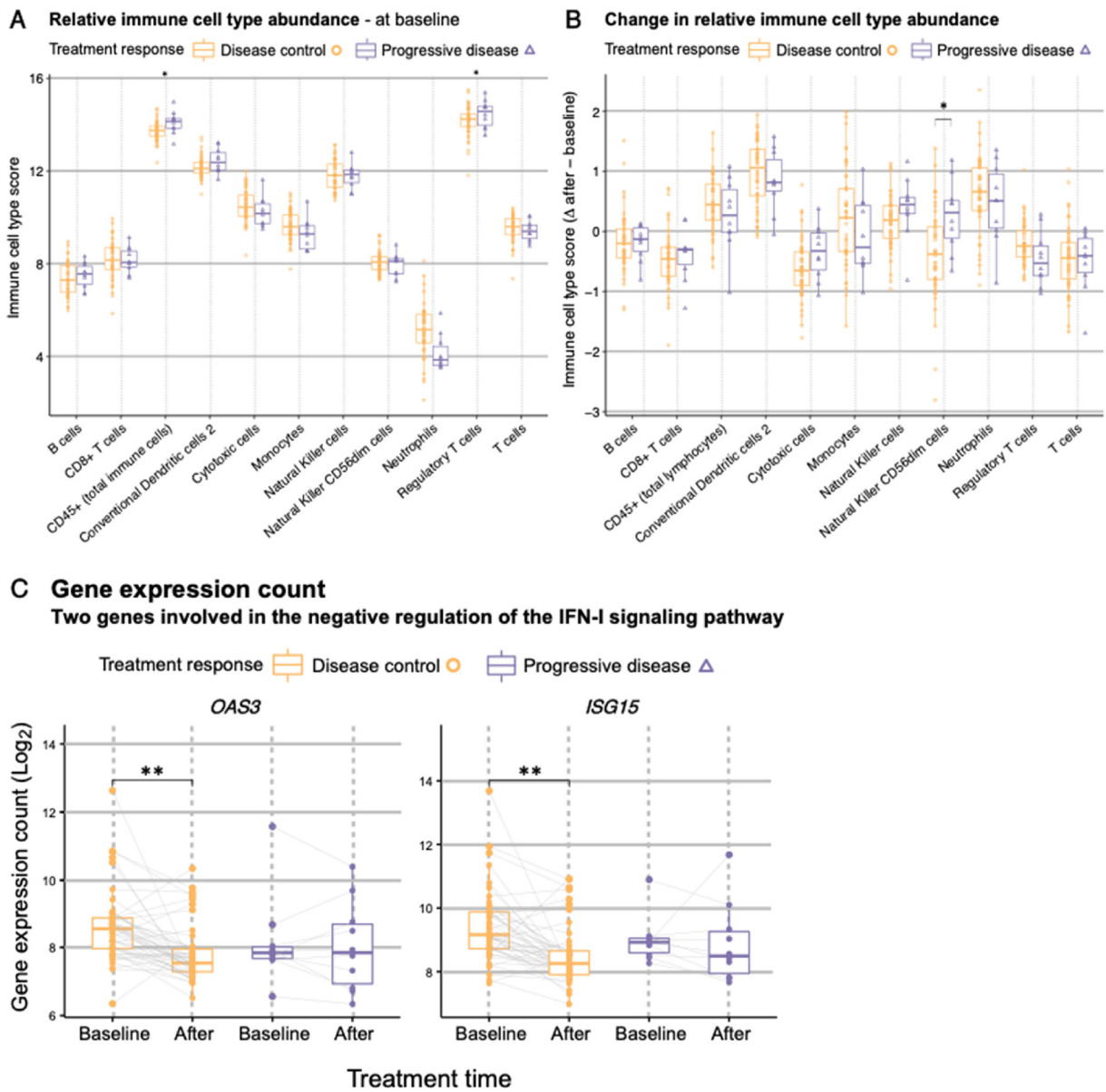


Fig. 4. Differences in immune profiles between disease control ($n = 48$, yellow) and progressive disease ($n = 10$, purple) patients. (A): Boxplots of samples at baseline displaying relative immune cell type abundances. (B): Boxplots of the change in relative immune cell type abundances after a single FOLFIRINOX cycle. (C): Boxplots of *OAS3* and *ISG15* expression counts (Log_2), involved in the negative regulation of the IFN-I signalling pathway, in baseline and after a single FOLFIRINOX cycle samples. Statistical significance: *BH.P < 0.05. Abbreviations: BH.P: Benjamin–Hochberg P value; FOLFIRINOX, 5-fluorouracil, folinic acid, irinotecan and oxaliplatin; IFN, interferon.

like receptor and tumour necrosis factor superfamily were enhanced after a single FOLFIRINOX cycle while the immune-associated pathways of antigen processing, B cell, NK cell, and T cell functions and cytotoxicity were diminished. Immune cell type analysis revealed alterations among all relative peripheral immune cell type abundances (BH.P < 0.05). The total immune cells (*PTPRC*, CD45⁺), cDC2, monocytes, NK cells and neutrophils increased while the B cells, cytotoxic cells, NK CD56^{dim} cells, total T cells, T regulatory (Treg) cells

and CD8⁺ T cells decreased after a single FOLFIRINOX cycle (Fig. 3D).

3.4. A single FOLFIRINOX cycle altered the expression of IC regulatory genes

The expression of the IC inhibitory genes *PDCD1* (PD-1), *CD274* (programmed death-ligand 1) and *PDCD1LG2* (PD-L2) were upregulated after a single FOLFIRINOX cycle compared to baseline with an

Table 2

The fourteen candidate genes selected for the FFX-ΔGEP score.

Gene	Disease control Mean (±SD)	Progressive disease Mean (±SD)	BH.P value	Weights
BID	0.030 (±0.48)	-0.237 (±0.42)	0.030	-1.63
FOXP3	0.012 (±0.67)	-0.518 (±0.43)	0.012	-0.10
KIR3DL1	0.018 (±0.59)	0.255 (±0.78)	0.018	0.26
KLRC1	0.035 (±0.56)	0.075 (±0.71)	0.035	0
KLRD1	0.044 (±0.46)	-0.293 (±0.53)	0.044	0
KLRG1	0.041 (±0.46)	-0.204 (±0.47)	0.041	0
MAF	0.023 (±0.44)	-0.111 (±0.47)	0.023	0.54
NFATC2	0.024 (±0.43)	-0.136 (±0.37)	0.024	0
PDGFRB	0.038 (±0.60)	0.011 (±0.49)	0.038	0.31
PLAU	0.043 (±0.99)	0.611 (±0.71)	0.043	0
REL	0.028 (±0.32)	0.278 (±0.37)	0.028	0
RRAD	0.008 (±0.46)	1.412 (±0.70)	0.008	0.97
SIGLEC1	0.020 (±0.84)	0.403 (±1.24)	0.020	0.21
TGFB2	0.020 (±0.64)	0.790 (±0.60)	0.020	0.81

The mean values of the Δ gene expression counts (±SD) per response group. The BH.P value between disease control and progressive disease patients. The assigned weights are calculated using LASSO multivariate regression analysis.

Abbreviations: SD: Standard Deviation; BH.P: Benjamin-Hochberg P value; LASSO: Least Absolute Shrinkage and Selection Operator.

average log₂ FOC of 1.1 (BH.P < 0.001). In contrast, the IC inhibitory genes BTLA, CTLA4 and its ligand CD86 (B7-2), HAVCR2 (TIM-3) and TIGIT were statistically significantly downregulated (BH.P < 0.001; Fig. 3E). The IC inhibitory gene LAG3 was not altered (Figure S4).

3.5. Subtle differences in the immune transcriptome of disease control and progressive disease patients after a single FOLFIRINOX cycle

Immune profiles of the disease control and progressive disease patients were compared at baseline and after a single FOLFIRINOX cycle. Baseline immune profiles revealed no differences in pathway activities between the two groups. However, a relatively high abundance of the total immune cells and Treg cells were observed in progressive disease patients (Fig. 4A). Immune profiles after a single FOLFIRINOX cycle revealed 400 DEGs in disease control and 256 DEGs in progressive disease patients (Figure S3), which were used in the ClueGo analysis based on the criteria in the materials and method section. Two key genes involved in the negative regulation of type-I interferon-mediated (IFN-1) signalling pathway were downregulated in disease control but not in progressive disease patients (BH.P < 0.01; Fig. 4C). The change in IC regulatory gene expression, pathway activity and immune cell type abundance was comparable in both groups (Figure S4), with one immune cell type exception. Driven by its solitary marker *KIR3DL1*, the relative abundance of NK CD56^{dim} cells was decreased in disease control but increased in progressive disease patients (BH.P < 0.05; Fig. 4B).

3.6. An eight-gene FFX-Δ GEP score predicted the lack of response after a single FOLFIRINOX cycle

To identify an early circulating biomarker that predicts the lack of FOLFIRINOX response, we developed an FFX-ΔGEP score. The Δ gene expression count, which results from subtracting the log₂ normalised gene expression counts of baseline samples from samples after a single FOLFIRINOX cycle, revealed fourteen candidate genes that differed significantly between disease control and progressive disease patients (BH.P < 0.05; Table 2). Least absolute shrinkage and selection operator multivariate regression analysis, which constructed the most optimal combination of candidate genes by assigning a regression coefficient (weight) to all candidate genes, was conducted. Six candidate genes were assigned a weight of zero and the FFX-ΔGEP score was composed of the remaining eight genes (Fig. 5):

FOLFIRINOX delta gene expression profiling

$$\begin{aligned} (\text{FFX } \Delta\text{GEP}) \text{ score} = & (0.26 * \text{KIR3DL1}) + (0.54 * \text{MAF}) \\ & + (0.31 * \text{PDGFRB}) + (0.97 * \text{RRAD}) + (0.21 * \text{SIGLEC1}) \\ & + (0.81 * \text{TGFB2}) - (1.63 * \text{BID}) - (0.10 * \text{FOXP3}) \end{aligned}$$

The eight-gene FFX-ΔGEP score ranged from 3.82 to -1.76 among all patients, and the performance to predict the lack of FOLFIRINOX response after a single cycle was assessed by ROC analysis (Fig. 6A). The leave-one-out cross-validated AUC (95% CI) was 0.87 (0.60–0.98), indicating that the FFX-ΔGEP score could distinguish between disease control and progressive disease patients. The predictive performance of the currently used absolute and proportional Δ CA19-9 values (95% CI) were 0.70 (0.27–1.0) and 0.52 (0.24–0.80). Importantly, the FFX-ΔGEP score outperformed Δ CA19-9 values with less overlap in the designation of disease control and progressive disease patients (Fig. 6B–D).

4. Discussion

In this study, we used paired blood samples of 68 patients with PDAC to investigate the effect of a single FOLFIRINOX cycle on the immune profile. We aimed to identify an early circulating biomarker to predict the lack of response to FOLFIRINOX. We revealed an eight-gene FFX-ΔGEP score that predicted the lack of FOLFIRINOX response only after the first cycle, independent of disease stage or change in CA19-9. This novel multigene FFX-ΔGEP score is, to our knowledge, the first gene expression-based early circulating biomarker predicting the lack of FOLFIRINOX response in patients with PDAC from all disease stages.

The FFX-ΔGEP score is composed of eight immune-related genes. Four of these genes (*FOXP3*, *KIR3DL1*, *MAF* and *SIGLEC1*) are associated with immune cell types [40–43], while the other four (*BID*, *PDGFRB*,

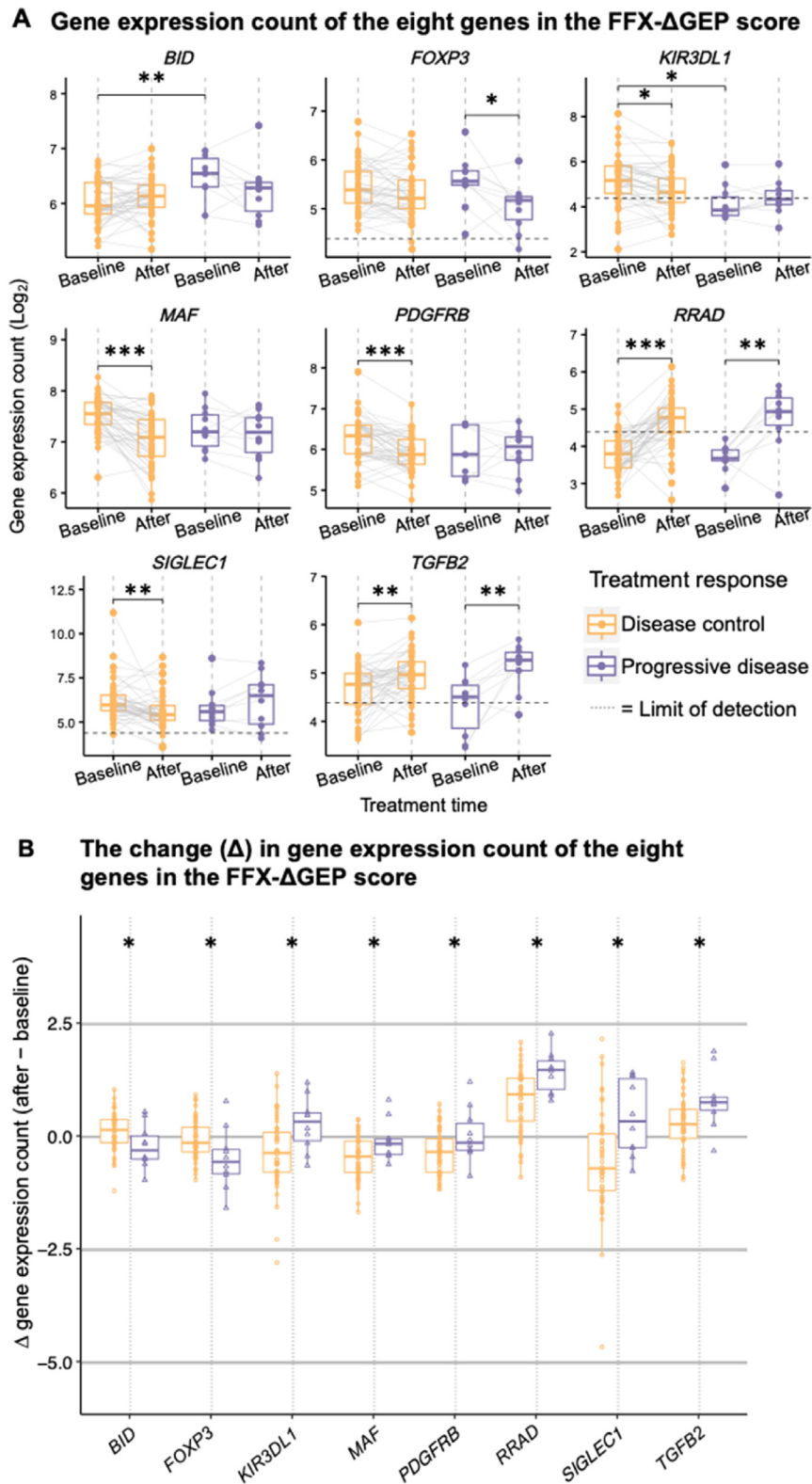


Fig. 5. **The eight genes that compose the FFX-ΔGEP score.** All boxplots compare disease control ($n = 48$, yellow) and progressive disease patients ($n = 10$, purple). **(A):** Boxplots of gene expression counts (Log_2) in baseline and after a single FOLFIRINOX cycle samples. **(B):** Boxplots of the change (Δ) in gene expression count after a single FOLFIRINOX cycle and baseline samples. Statistical significance: * BH.P < 0.05, ** BH.P < 0.01, *** BH.P < 0.001. Abbreviations: BH.P: Benjamin–Hochberg P value; FFX-Δ GEP: FOLFIRINOX-delta gene expression profiling; FOLFIRINOX, 5-fluorouracil, folinic acid, irinotecan and oxaliplatin.

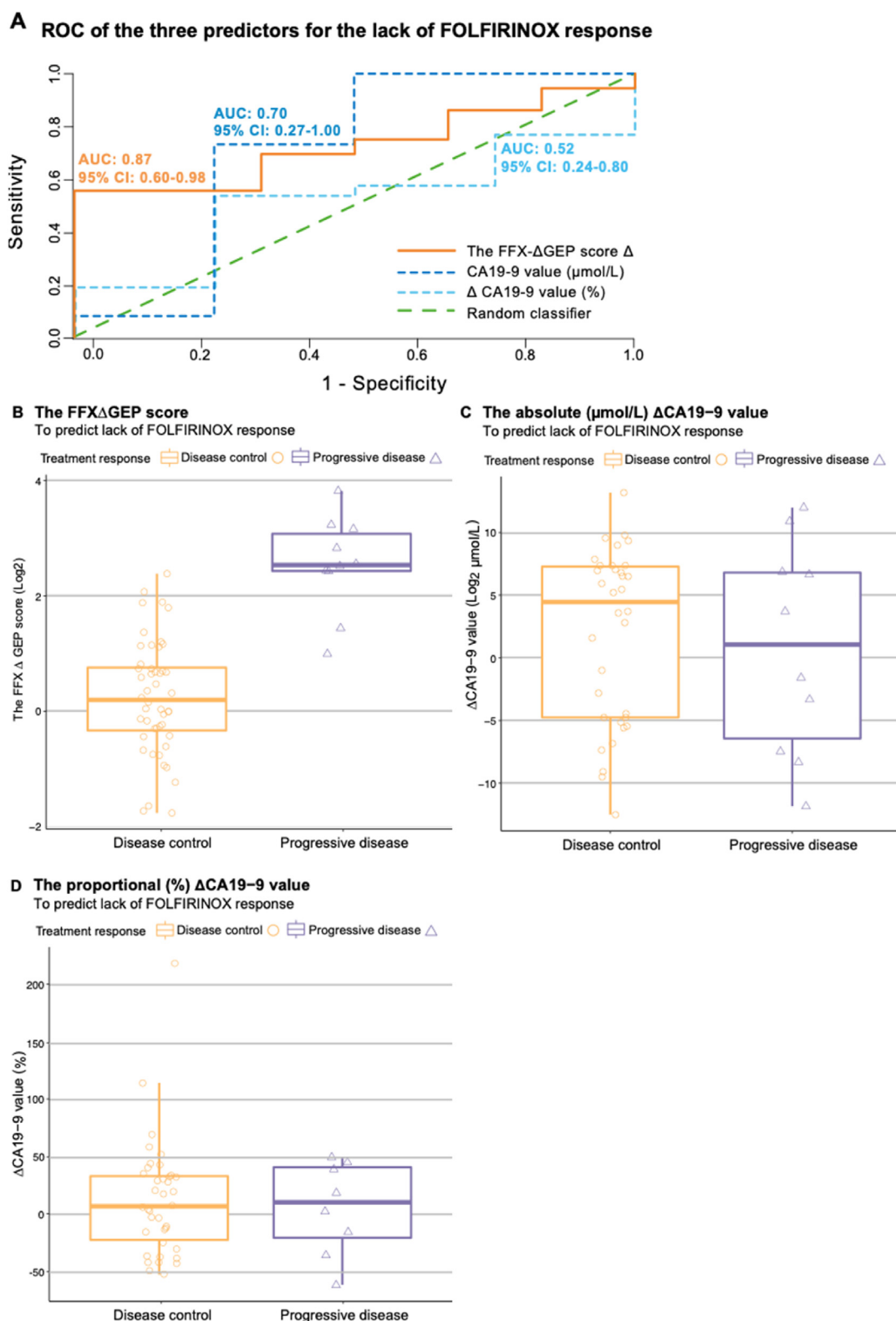


Fig. 6. **The FFX- Δ GEP score.** (A): The ROC of the FFX- Δ GEP score (orange), absolute ($\mu\text{mol/L}$) \log_2 Δ CA19-9 score (dark blue), proportional (%) Δ CA19-9 score (light blue), and the random classifier (green). (B–D): Boxplots of the FFX- Δ GEP score (B), the absolute ($\mu\text{mol/L}$) \log_2 Δ CA19-9 score (C) and the proportional (%) Δ CA19-9 score (D) for disease control ($n = 48$, yellow) and progressive disease ($n = 10$, purple) patients. *Abbreviations* AUC: Area Under the Curve; CA19-9: carbohydrate antigen 19-9; CI: confidence interval; FFX- Δ GEP: FOLFIRINOX-delta gene expression profiling; FOLFIRINOX, 5-fluorouracil, folinic acid, irinotecan and oxaliplatin; ROC: receiver operating characteristic.

RRAD and *TGFB2*) are associated with the tumour or chemotherapeutic efficacy [44–47]. *FOXP3*, a marker for Tregs, is associated with poor PDAC prognosis [40,48] but their peripheral abundance could be reduced by neoadjuvant FOLFIRINOX [49,50]. *KIR3DL1* inhibits NK cell activity [41] and is associated with PDAC progression [51]. In this study, *KIR3DL1* expression decreased indeed only in disease control patients. *MAF* is a transcription factor that can impair CD8 T cell function [42] and is often highly expressed in M2 macrophages [52], which are associated with poor prognosis in PDAC [53]. Correspondingly, our results showed a decrease in *MAF* expression in disease control patients only. *SIGLEC1* is a protein that mediates phagocytosis and endocytosis [54] and is expressed in the blood by activated CD14⁺ monocytes in reaction to IFN- γ [43,55]. In contrast, our results showed downregulation of *SIGLEC1* but increased activation of the IFN- γ pathway in disease control patients. *BID* encodes pro-apoptotic proteins [44] and their deregulated expression is associated with apoptotic resistance in PDAC [56]. Accordingly, our results showed downregulation in *BID* expression in progressive disease patients only. *PDGFRB* is associated with poor disease-free survival, cancer cell invasion and metastasis in PDAC [45,46]. These pro-tumoural effects are in line with our results showing no change in *PDGFRB* expression in progressive disease but downregulation in disease control patients. In gastric and colorectal cancer, 5-FU and oxaliplatin, two chemotherapeutic agents of FOLFIRINOX, displayed increased efficacy when combined with *RRAD* inhibition [57]. Transforming growth factor- β 2 (*TGFB2*) plays a complex role in PDAC and can both promote and inhibit tumour growth [58,59].

This study has some limitations. First, our FFX- Δ GEP score needs to be validated in a larger cohort of patients because the current sample was not sufficient to accurately calculate a cut-off value for the response or lack of response to FOLFIRINOX treatment. Second, the patients in this study received FOLFIRINOX in combination with G-CSF, but it would have been ideal to also include a patient group who received FOLFIRINOX only. However, at least in the Netherlands, the combination of G-CSF and FOLFIRINOX is standard practice due to the high risk of neutropenia. Therefore, we have accepted this omission and did not evaluate the performance of the FFX- Δ GEP score in patients who did not receive G-CSF. Third, we did not evaluate the specificity of the FFX- Δ GEP score for FOLFIRINOX by comparing its predictive ability in a control cohort of patients treated with another chemotherapy regimen, such as Nab-Paclitaxel-Gemcitabine. While this would have been ideal, the availability of patients treated with these regimens is limited due to the superior effectiveness of FOLFIRINOX. However, we plan to conduct a multicenter clinical trial to validate our results. Lastly, treatment response was evaluated using CT scans, but

some patients experience prolonged OS without showing an imaging response. Therefore, it is important to determine whether the FFX- Δ GEP score can predict FOLFIRINOX-induced prolonged OS.

To our knowledge, this study is the first to describe the effect of a single FOLFIRINOX cycle, in combination with G-CSF, on the immune transcriptome of patients with PDAC. We discovered that this treatment significantly changed the expression of 395 immune-related genes, even after two weeks of recovery. Our results showed that the relative peripheral abundance of total immune cells (CD45⁺), B cells, cDC2, cytotoxic cells, monocytes, NK CD56^{dim} cells and all T cell subsets (total, CD8⁺ and Treg) were reduced while the relative neutrophil abundance was increased after a single cycle of treatment. The increase in granulocyte-derived cells could be due to G-CSF which can affect the relative abundance of the other immune cells. In line with our results, previous studies described a rapid recovery of total lymphocytes, cDCs and monocytes after two weeks of chemotherapy [47,60] and increased cDC2s after G-CSF treatment [61].

Importantly, the immune transcriptome in patients with different disease stages or different baseline CA19-9 values was similar. This suggests that the progression of PDAC does not stimulate the systemic immune response. Additionally, we could not predict the lack of FOLFIRINOX response using baseline samples only. This highlights the challenges we face in applying precision medicine protocols or stratifying PDAC patients to receive their most suitable treatment. Based on our results, at least one cycle of FOLFIRINOX is needed to predict the lack of response in patients with PDAC.

5. Conclusions

In this study, we developed a novel multigene FFX- Δ GEP score using targeted immune-gene expression profiling and found that it could predict the lack of FOLFIRINOX response in patients having pancreatic cancer after only one cycle. In our cohort, the FFX- Δ GEP score predicted the lack of FOLFIRINOX response with more accuracy than the absolute or proportional change in CA19-9 levels. In addition, we were the first to describe the pronounced effect of a single FOLFIRINOX cycle on the immune transcriptome in the blood of patients with PDAC from all disease stages. Further research is needed to validate our results in a larger cohort of patients, preferably including those who did not receive G-CSF treatment or were treated with another type of chemotherapeutic regimen.

Financial support

This work was financially supported by the Survival with Pancreatic Cancer Foundation (www.supportcasper.nl) [grant number OVIT17-06].

Author contributions

Casper W. van Eijck: conceptualization, methodology, formal analysis, investigation, writing – original draft, visualization. *Willem de Koning*: software, formal analysis, writing – review & editing. *Fleur van der Sijde*: investigation, resources, writing – review & editing. *Miranda Moskie*: resources, writing – review & editing. *Bas Groot Koerkamp*: investigation, resources, writing – review & editing, project administration. *Marjolein Homs*: resources, writing – review & editing. *Sjoerd van der Burg*: conceptualization, writing – review & editing. *Casper H. van Eijck*: conceptualization, methodology, writing – review & editing, supervision, project administration. *Dana Mustafa*: conceptualization, methodology, data curation, writing – review & editing, supervision.

Ethics approval and consent to participate

Participating patients in this study were included in two trials conducted according to the guidelines of the Declaration of Helsinki and approved by the Ethics Committees of Erasmus MC (ethics committee reference number MEC-2018-087 and MEC-2018-004). Written informed consent was obtained from all patients.

Availability of data and materials

The datasets used and/or analysed during the current study are available, with permission of the Erasmus Medical Center Rotterdam, from the corresponding author on reasonable request.

Conflict of interest statement

The authors declare that they have no competing interests.

Acknowledgements

The authors would like to give special thanks to all students involved in the blood collection, to Disha S. Vadgama and Jasper Dumas for their help in processing the blood samples, and to Jie Ju for her assistance with the LASSO multivariate regression analysis.

Appendix A. Supplementary data

Supplementary data to this article can be found online at <https://doi.org/10.1016/j.ejca.2022.12.024>.

References

- [1] Sarantis P, Koustas E, Papadimitropoulou A, Papavassiliou AG, Karamouzis MV. Pancreatic ductal adenocarcinoma: treatment hurdles, tumor microenvironment and immunotherapy. *World J Gastrointest Oncol* 2020;12:173–81.
- [2] Sung H, Ferlay J, Siegel RL, Laversanne M, Soerjomataram I, Jemal A, et al. Global cancer statistics 2020: GLOBOCAN estimates of incidence and mortality worldwide for 36 cancers in 185 countries. *CA Cancer J Clin* 2021;71:209–49.
- [3] Rangarajan K, Pucher PH, Armstrong T, Bateman A, Hamady Z. Systemic neoadjuvant chemotherapy in modern pancreatic cancer treatment: a systematic review and meta-analysis. *Ann R Coll Surg Engl* 2019;101:453–62.
- [4] Kikuyama M, Kamisawa T, Kuruma S, Chiba K, Kawaguchi S, Terada S, et al. Early diagnosis to improve the poor prognosis of pancreatic cancer. *Cancers* 2018;10.
- [5] Adamska A, Domenichini A, Falasca M. Pancreatic ductal adenocarcinoma: current and evolving therapies. *Int J Mol Sci* 2017;18.
- [6] Fan JQ, Wang MF, Chen HL, Shang D, Das JK, Song J. Current advances and outlooks in immunotherapy for pancreatic ductal adenocarcinoma. *Mol Cancer* 2020;19:32.
- [7] Wolfgang CL, Herman JM, Laheru DA, Klein AP, Erdek MA, Fishman EK, et al. Recent progress in pancreatic cancer. *CA Cancer J Clin* 2013;63:318–48.
- [8] van der Sijde F, van Dam JL, Groot Koerkamp B, Haberkorn BCM, Homs MYV, Mathijssen D, et al. Treatment response and conditional survival in advanced pancreatic cancer patients treated with FOLFIRINOX: a multicenter cohort study. *JAMA Oncol* 2022;2022:8549487.
- [9] Suker M, Beumer BR, Sadot E, Marthey L, Faris JE, Mellon EA, et al. FOLFIRINOX for locally advanced pancreatic cancer: a systematic review and patient-level meta-analysis. *Lancet Oncol* 2016;17:801–10.
- [10] Conroy T, Desseigne F, Ychou M, Bouche O, Guimbaud R, Becouarn Y, et al. FOLFIRINOX versus gemcitabine for metastatic pancreatic cancer. *N Engl J Med* 2011;364:1817–25.
- [11] Conroy T, Hammel P, Hebbar M, Ben Abdelghani M, Wei AC, Raoul JL, et al. FOLFIRINOX or gemcitabine as adjuvant therapy for pancreatic cancer. *N Engl J Med* 2018;379:2395–406.
- [12] Janssen QP, Buettner S, Suker M, Beumer BR, Addeo P, Bachellier P, et al. Neoadjuvant FOLFIRINOX in patients with borderline resectable pancreatic cancer: a systematic review and patient-level meta-analysis. *J Natl Cancer Inst* 2019;111:782–94.
- [13] Perri G, Prakash L, Qiao W, Varadhachary GR, Wolff R, Fogelman D, et al. Response and survival associated with first-line FOLFIRINOX vs gemcitabine and nab-paclitaxel chemotherapy for localized pancreatic ductal adenocarcinoma. *JAMA Surg* 2020;155:832–9.
- [14] Thibodeau S, Voutsadakis IA. FOLFIRINOX chemotherapy in metastatic pancreatic cancer: a systematic review and meta-analysis of retrospective and phase II studies. *J Clin Med* 2018;7.
- [15] Richards MK, Liu F, Iwasaki H, Akashi K, Link DC. Pivotal role of granulocyte colony-stimulating factor in the development of progenitors in the common myeloid pathway. *Blood* 2003;102:3562–8.
- [16] Steger G, Pichler P, Airoidi M, Mazza P, Fontaine C, Timmer Bonte J, et al. 1697P - use of lipegfilgrastim for the prophylaxis of chemotherapy-induced neutropenia: pan-European non-interventional study. *Ann Oncol* 2018;29. viii607–viii8.
- [17] Terazawa T, Goto M, Miyamoto T, Asaishi K, Shimamoto F, Kuwakado S, et al. Efficacy of prophylactic G-CSF in patients receiving FOLFIRINOX: a preliminary retrospective study. *Intern Med* 2015;54:2969–73.
- [18] Timmer-Bonte JNH, Ouwkerk J, Faber LM, Kerkhofs LGM, Laterveer L, Ten Oever D, et al. Lipegfilgrastim for prophylaxis of chemotherapy-induced neutropenia in Dutch patients. *Neth J Med* 2020;78:270–6.

- [19] Winter JM, Yeo CJ, Brody JR. Diagnostic, prognostic, and predictive biomarkers in pancreatic cancer. *J Surg Oncol* 2013;107:15–22.
- [20] van der Sijde F, Vietsch EE, Mustafa DAM, Besselink MG, Groot Koerkamp B, van Eijck CHJ. Circulating biomarkers for prediction of objective response to chemotherapy in pancreatic cancer patients. *Cancers* 2019;11.
- [21] Principe DR, Narbutis M, Kumar S, Park A, Viswakarma N, Dorman MJ, et al. Long-term gemcitabine treatment reshapes the pancreatic tumor microenvironment and sensitizes murine carcinoma to combination immunotherapy. *Cancer Res* 2020;80:3101–15.
- [22] Zhou C, Chen G, Huang Y, Zhou J, Lin L, Feng J, et al. Camrelizumab plus carboplatin and pemetrexed versus chemotherapy alone in chemotherapy-naïve patients with advanced non-squamous non-small-cell lung cancer (CameL): a randomised, open-label, multicentre, phase 3 trial. *Lancet Respir Med* 2021;9:305–14.
- [23] Park SJ, Ye W, Xiao R, Silvín C, Padgett M, Hodge JW, et al. Cisplatin and oxaliplatin induce similar immunogenic changes in preclinical models of head and neck cancer. *Oral Oncol* 2019;95:127–35.
- [24] Bezu L, Gomes-de-Silva LC, Dewitte H, Breckpot K, Fucikova J, Spisek R, et al. Combinatorial strategies for the induction of immunogenic cell death. *Front Immunol* 2015;6:187.
- [25] Tesniere A, Schlemmer F, Boige V, Kepp O, Martins I, Ghiringhelli F, et al. Immunogenic death of colon cancer cells treated with oxaliplatin. *Oncogene* 2010;29:482–91.
- [26] Liu WM, Fowler DW, Smith P, Dalgleish AG. Pre-treatment with chemotherapy can enhance the antigenicity and immunogenicity of tumours by promoting adaptive immune responses. *Br J Cancer* 2010;102:115–23.
- [27] Stojanovska V, Prakash M, McQuade R, Fraser S, Apostolopoulos V, Sakkal S, et al. Oxaliplatin treatment alters systemic immune responses. *BioMed Res Int* 2019;2019:4650695.
- [28] Lyman GH, Yau L, Nakov R, Krendyukov A. Overall survival and risk of second malignancies with cancer chemotherapy and G-CSF support. *Ann Oncol* 2018;29:1903–10.
- [29] Eisenhauer EA, Therasse P, Bogaerts J, Schwartz LH, Sargent D, Ford R, et al. New response evaluation criteria in solid tumours: revised RECIST guideline (version 1.1). *Eur J Cancer* 2009;45:228–47.
- [30] van der Sijde F, Li Y, Schraauwen R, de Koning W, van Eijck CHJ, Mustafa DAM. RNA from stabilized whole blood enables more comprehensive immune gene expression profiling compared to RNA from peripheral blood mononuclear cells. *PLoS One* 2020;15:e0235413.
- [31] Cesano A. nCounter(R) PanCancer immune profiling panel (NanoString technologies, Inc., seattle, WA). *J Immunother Cancer* 2015;3:42.
- [32] Geiss GK, Bumgarner RE, Birditt B, Dahl T, Dowidar N, Dunaway DL, et al. Direct multiplexed measurement of gene expression with color-coded probe pairs. *Nat Biotechnol* 2008;26:317–25.
- [33] Vandesompele J, De Preter K, Pattyn F, Poppe B, Van Roy N, De Paeppe A, et al. Accurate normalization of real-time quantitative RT-PCR data by geometric averaging of multiple internal control genes. *Genome Biol* 2002;3. research0034.1.
- [34] NanoString Technologies®. I. nCounter Advanced Analysis 2.0 User Manual. 2018. Seattle, Washington.
- [35] de Koning W, Latifi D, Li Y, van Eijck CHJ, Stubbs AP, Mustafa DAM. Identification, validation, and utilization of immune cells in pancreatic ductal adenocarcinoma based on marker genes. *Front Immunol* 2021;12:649061.
- [36] Bindea G, Mlecnik B, Hackl H, Charoentong P, Tosolini M, Kirilovsky A, et al. ClueGO: a Cytoscape plug-in to decipher functionally grouped gene ontology and pathway annotation networks. *Bioinformatics* 2009;25:1091–3.
- [37] Team RC. R: A language and environment for statistical computing. Vienna, Austria: R Foundation for Statistical Computing; 2021.
- [38] Wickham H. ggplot2: elegant graphics for data analysis. New York: Springer-Verlag; 2016.
- [39] Blighe K, Rana S, Lewis M. EnhancedVolcano: publication-ready volcano plots with enhanced colouring and labeling. 2022.
- [40] Hu L, Zhu M, Shen Y, Zhong Z, Wu B. The prognostic value of intratumoral and peritumoral tumor-infiltrating FoxP3+Treg cells in of pancreatic adenocarcinoma: a meta-analysis. *World J Surg Oncol* 2021;19:300.
- [41] Peng YP, Zhu Y, Zhang JJ, Xu ZK, Qian ZY, Dai CC, et al. Comprehensive analysis of the percentage of surface receptors and cytotoxic granules positive natural killer cells in patients with pancreatic cancer, gastric cancer, and colorectal cancer. *J Transl Med* 2013;11:262.
- [42] Speiser DE, Ho PC, Verdeil G. Regulatory circuits of T cell function in cancer. *Nat Rev Immunol* 2016;16:599–611.
- [43] Oliveira JJ, Karrar S, Rainbow DB, Pinder CL, Clarke P, Rubio Garcia A, et al. The plasma biomarker soluble SIGLEC-1 is associated with the type I interferon transcriptional signature, ethnic background and renal disease in systemic lupus erythematosus. *Arthritis Res Ther* 2018;20:152.
- [44] Adams JM, Cory S. Bcl-2-regulated apoptosis: mechanism and therapeutic potential. *Curr Opin Immunol* 2007;19:488–96.
- [45] Singh PK, Wen Y, Swanson BJ, Shanmugam K, Kazlauskas A, Cerny RL, et al. Platelet-derived growth factor receptor beta-mediated phosphorylation of MUC1 enhances invasiveness in pancreatic adenocarcinoma cells. *Cancer Res* 2007;67:5201–10.
- [46] Weissmueller S, Machado E, Saborowski M, Morris JPT, Wagenblast E, Davis CA, et al. Mutant p53 drives pancreatic cancer metastasis through cell-autonomous PDGF receptor beta signaling. *Cell* 2014;157:382–94.
- [47] Bang S, Kim HS, Choo YS, Park SW, Chung JB, Song SY. Differences in immune cells engaged in cell-mediated immunity after chemotherapy for far advanced pancreatic cancer. *Pancreas* 2006;32:29–36.
- [48] Ino Y, Yamazaki-Itoh R, Shimada K, Iwasaki M, Kosuge T, Kanai Y, et al. Immune cell infiltration as an indicator of the immune microenvironment of pancreatic cancer. *Br J Cancer* 2013;108:914–23.
- [49] Peng H, James CA, Cullinan DR, Hogg GD, Mudd JL, Zuo C, et al. Neoadjuvant FOLFIRINOX therapy is associated with increased effector T cells and reduced suppressor cells in patients with pancreatic cancer. *Clin Cancer Res* 2021;27:6761–71.
- [50] Michelakos T, Cai L, Villani V, Sabbatino F, Kontos F, Fernandez-Del Castillo C, et al. Tumor microenvironment immune response in pancreatic ductal adenocarcinoma patients treated with neoadjuvant therapy. *J Natl Cancer Inst* 2021;113:182–91.
- [51] Lee HS, Leem G, Kang H, Jo JH, Chung MJ, Jang SJ, et al. Peripheral natural killer cell activity is associated with poor clinical outcomes in pancreatic ductal adenocarcinoma. *J Gastroenterol Hepatol* 2021;36:516–22.
- [52] Kang K, Park SH, Chen J, Qiao Y, Giannopoulou E, Berg K, et al. Interferon-gamma represses M2 gene expression in human macrophages by disassembling enhancers bound by the transcription factor MAF. *Immunity* 2017;47:235–250 e4.
- [53] Yang S, Liu Q, Liao Q. Tumor-associated macrophages in pancreatic ductal adenocarcinoma: origin, polarization, function, and reprogramming. *Front Cell Dev Biol* 2020;8:607209.
- [54] O'Neill AS, van den Berg TK, Mullen GE. Sialoadhesin - a macrophage-restricted marker of immunoregulation and inflammation. *Immunology* 2013;138:198–207.
- [55] Xiong YS, Cheng Y, Lin QS, Wu AL, Yu J, Li C, et al. Increased expression of Siglec-1 on peripheral blood monocytes and its role in mononuclear cell reactivity to autoantigen in rheumatoid arthritis. *Rheumatology* 2014;53:250–9.

- [56] Campani D, Esposito I, Boggi U, Cecchetti D, Menicagli M, De Negri F, et al. Bcl-2 expression in pancreas development and pancreatic cancer progression. *J Pathol* 2001;194:444–50.
- [57] Kim HK, Lee I, Kim ST, Lee J, Kim KM, Park JO, et al. RRAD expression in gastric and colorectal cancer with peritoneal carcinomatosis. *Sci Rep* 2019;9:19439.
- [58] Chen J, Ding ZY, Li S, Liu S, Xiao C, Li Z, et al. Targeting transforming growth factor-beta signaling for enhanced cancer chemotherapy. *Theranostics* 2021;11:1345–63.
- [59] Murphy JE, Wo JY, Ryan DP, Clark JW, Jiang W, Yeap BY, et al. Total Neoadjuvant Therapy With FOLFIRINOX in Combination With Losartan Followed by Chemoradiotherapy for Locally Advanced Pancreatic Cancer: a Phase 2 Clinical Trial. *JAMA Oncol* 2019;5:1020–7.
- [60] Markowicz S, Walewski J, Zajda K, Wiechno PJ, Skurzak HM, Giermek J, et al. Recovery of dendritic cell counts and function in peripheral blood of cancer patients after chemotherapy. *Cytokines Cell Mol Ther* 2002;7:15–24.
- [61] Bonanno G, Procoli A, Mariotti A, Corallo M, Perillo A, Danese S, et al. Effects of pegylated G-CSF on immune cell number and function in patients with gynecological malignancies. *J Transl Med* 2010;8:114.